INTERNATIONAL JOURNAL OF ADAPTIVE CONTROL AND SIGNAL PROCESSING
Int. J. Adapt. Control Signal Process. 2015; **00**:1–21
Published online in Wiley InterScience (www.interscience.wiley.com). DOI: 10.1002/acs

Direct and indirect adaptive integral line-of-sight path-following controllers for marine craft exposed to ocean currents

Thor I. Fossen[1]* and Anastasios M. Lekkas[2]

[1]*Centre for Autonomous Marine Operations and Systems (AMOS), Department of Engineering Cybernetics, Norwegian University of Science and Technology, Trondheim, Norway*
[2]*Centre for Autonomous Marine Operations and Systems (AMOS), Department of Marine Technology, Norwegian University of Science and Technology, Trondheim, Norway*

SUMMARY

We present a direct and an indirect nonlinear adaptive path-following controller for marine craft based on a line-of-sight (LOS) guidance principle used by ancient navigators. The control laws are implemented using hydro-acoustic relative velocity measurements as opposed to absolute velocity measurements. For this purpose a kinematic model for relative velocity in *amplitude-phase form* is derived. The first contribution is an adaptive indirect controller based on a disturbance observer designed for estimation and compensation of ocean currents. The equilibrium points of the cross-track and parameter estimation errors are proven to be globally κ-exponentially stable. This guarantees that the estimated drift term converges to its true value exponentially. The observer is used in conjuncture with a control law to obtain asymptotic tracking and path following in presence of ocean currents. The second contribution is a direct adaptive integral LOS controller for path following. Global convergence of the cross-track error is proven by using Barbălat's lemma, which ensures that the parameter estimation error is bounded. Both methods can be applied to the horizontal-plane motion of surface vessels and autonomous underwater vehicles (AUVs). An AUV case study is included to verify the results. Copyright © 2015 John Wiley & Sons, Ltd.

Received ...

KEY WORDS: Adaptive control; guidance systems; marine systems; autonomous vehicles; kinematics.

1. INTRODUCTION

Ships and underwater vehicles rely heavily on guidance systems in order to accomplish desired motion control scenarios such as object tracking, path following, path tracking and path maneuvering; see Breivik et al. [3], Breivik [4] and Yanushevsky [26] for instance. In three degrees of freedom (DOF) path-following applications, the control objective is to follow a predefined planar path without needing to set time constraints. A popular and effective way to achieve convergence to the desired path is to implement a lookahead-based LOS guidance law mimicking an experienced sailor. This method exploits the geometry of the problem and generates a reference trajectory for the yaw angle, which is fed into the heading autopilot. Guided LOS motion control of AUVs using sliding mode control for stabilizing the combined speed, steering and diving responses was addressed by Healey and Lienard [16]. An implementation of the LOS guidance law for straight-line path following can be found in Fossen [10], whereas in Breivik and Fossen [5] the method was implemented for path following of curved paths. Planar path-following controllers for underactuated marine vehicles using polar-like kinematic models have been investigated by Aicardi et al. [2].

*Correspondence to: Thor I. Fossen, Department of Engineering Cybernetics, Norwegian University of Science and Technology, 7491 Trondheim, Norway. E-mail: fossen@ieee.org

Path-following methods for underactuated vehicles in the presence of large modeling parametric uncertainty using adaptive supervisory control that combines logic-based switching with Lyapunov-based techniques are discussed by Aguiar and Hespanha [1]. An alternative model-based approach for robust adaptive path following is proposed by Do et al. [9]. Complexity drastically increases if speed and heading are stabilized simultaneously, see Lapierre et al. [19] and Skjetne et al. [24] for instance. In this paper we assume that the vehicle's speed is measured and derive a adaptive LOS guidance law for path following and compensation of drift forces. An overview of the LOS guidance principles are given by Fossen [11].

Despite the effectiveness and simplicity of *proportional* (P) guidance laws they have limitations when the vehicle is exposed to unknown *drift forces* caused by waves, wind and ocean currents. Underactuated ocean vehicles only control speed and heading in the horizontal plane. Hence, convergence to a curved path under the influence of an unknown drift force is non-trivial. Such vehicles will exhibit large cross-track errors during path following and in steady state, which depends on the path curvature as well as the direction and strength of the drift force. It is then necessary to modify the LOS guidance law to include integral action. This is referred to as *proportional-integral* (PI) guidance. Breivik and Fossen [6] showed that PI guidance laws could eliminate the steady-state cross-track error for straight-line path following. However, no stability results were provided. A far more sophisticated approach was presented by Børhaug et al. [7] in which the *nominal system* was proven globally κ-exponentially stable for straight-line path following and constant forward speed. In addition the cascade of the motion controller and the PI guidance law guarantees asymptotic tracking. A similar approach based on relative velocity was presented by Caharija et al. [8].

The main result of the paper is a conceptual new integral LOS guidance law based on adaptive control theory, which effectively compensate for drift forces due to waves, wind and ocean currents. The structure of the adaptive integral LOS guidance law is different from the well established integral LOS controller of Børhaug et al. [7]. The adaptive integral LOS guidance law is used in cascade with a nonlinear PID heading autopilot and global κ-exponential stability and global convergence are proven for the indirect and direct adaptive control laws, respectively. The PI guidance laws are intuitive and easy to implement since they are formulated at a kinematic level without using the vehicle parameters. Parametric uncertainty is dealt with by using a sliding mode controller for tracking of the desired heading angle generated by the integral LOS guidance law. Both guidance laws can be used for curved paths and time-varying speed. The adaptive integral LOS controllers rely upon a reformulated kinematic expression for the cross-track error using the concept of relative velocity. Hence, relative velocity measurements from hydro-acoustic reference systems can be used when implementing the control laws. It is also possible to modify the adaptation law to use absolute velocity measurements (Fossen et al. [12]).

2. KINEMATICS

We will consider a marine craft that is assigned to converge to a 2-D parametrized path specified by straight lines or curves (see Figure 1). 2-D paths are commonly used for surface vessels, while for underwater vehicles it is assumed that the depth is controlled independently such that the path-following control problem is limited to motions in the horizontal plane. Without loss of generality, the presented methods can be extended to 3-D motions by following a similar approach as Lekkas and Fossen [20].

2.1. Cross-track error

A 2-D continuous $\mathcal{C}^1$ parametrized path $(x_p(\theta), y_p(\theta))$ where $\theta \geq 0$ denotes the path variable is assumed to go through a set of successive waypoints (x_j, y_j) for $j = 1, ..., N$ as illustrated in Figure 1. The path variable θ propagates according to (Fossen [11]):

$$\dot{\theta} = \frac{U}{\sqrt{x_p'(\theta)^2 + y_p'(\theta)^2}} > 0 \tag{1}$$

DOI: 10.1002/acs

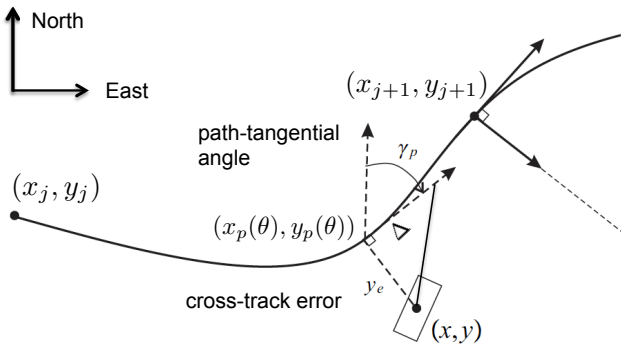

Figure 1. LOS guidance geometry where Δ is the lookahead distance tangential to the path and y_e is the cross-track error normal to the path. The angle γ_p denotes the rotation angle from the NED reference frame to the path-tangential reference frame.

where $x'_p(\theta) = \partial x_p/\partial\theta$ and $y'_p(\theta) = \partial y_p/\partial\theta$. The path-tangential reference frame is rotated an angle $\gamma_p(\theta)$ from the North-East-Down (NED) reference frame using the rotation matrix:

$$\mathbf{R}(\gamma_p(\theta)) = \begin{bmatrix} \cos(\gamma_p(\theta)) & -\sin(\gamma_p(\theta)) \\ \sin(\gamma_p(\theta)) & \cos(\gamma_p(\theta)) \end{bmatrix} \in SO(2) \tag{2}$$

Consequently, the cross-track error satisfies:

$$\begin{bmatrix} 0 \\ y_e \end{bmatrix} = \mathbf{R}^\top(\gamma_p(\theta)) \begin{bmatrix} x - x_p(\theta) \\ y - y_p(\theta) \end{bmatrix} \tag{3}$$

Expanding (3) gives the normal line:

$$y - y_p(\theta) = -\frac{1}{\tan(\gamma_p(\theta))}(x - x_p(\theta)) \tag{4}$$

through $(x_p(\theta), y_p(\theta))$ and the cross-track error:

$$y_e = -(x - x_p(\theta))\sin(\gamma_p(\theta)) + (y - y_p(\theta))\cos(\gamma_p(\theta)) \tag{5}$$

The path-tangential angle is given by:

$$\gamma_p(\theta) = \text{atan2}\left(y'_p(\theta), x'_p(\theta)\right) \tag{6}$$

where $\text{atan2}(y, x)$ is the angle between the positive x-axis of a plane and the point given by the coordinates (x, y) on it. For a straight line between two waypoints $\gamma_p = \text{atan2}(y_{j+1} - y_j, x_{j+1} - x_j)$ is constant, while for a curved parametrized path $\gamma_p(\theta)$ will vary according to (6).

As pointed out by Samson [23] there may be infinite solutions of (4) when solving for θ if the path is a closed curve. In the following we will assume that the path is an open curve, i.e. the end point is different from the start point. Similar as Fossen and Pettersen [13], we define the unique solution $y_e(\theta^*)$ of (4) by:

$$\theta^* := \arg\min_{\theta \geq 0} \left\{ \frac{U^2}{x'_p(\theta)^2 + y'_p(\theta)^2} \right\} \quad \text{subject to (4)} \tag{7}$$

which minimizes $\dot{\theta}$ given by (1). This is a nonlinear optimization problem, which can be solved numerically. However, for many paths θ^* can be found by computing all possible projection candidates θ_i $(i = 1, \ldots, M)$ given by (4) and choose the one closest to the previous θ^*-value.

DOI: 10.1002/acs

2.2. Equations of relative motion

The kinematic equations can be expressed in terms of the relative *surge* and *sway* velocities $u_r = u - u_c$ and $v_r = v - v_c$ according to Fossen [14]:

$$\dot{x} = u_r \cos(\psi) - v_r \sin(\psi) + V_x \tag{8}$$

$$\dot{y} = u_r \sin(\psi) + v_r \cos(\psi) + V_y \tag{9}$$

$$\dot{\psi} = r \tag{10}$$

where ψ and r are the yaw angle and rate, respectively. Let the pair (u_c, v_c) denote the body-fixed current velocities in surge and sway. Hence, the North-East current velocities (V_x, V_y) are given by:

$$[V_x, V_y]^\top = \mathbf{R}(\psi)[u_c, v_c]^\top, \quad \mathbf{R}(\psi) = \begin{bmatrix} \cos(\psi) & -\sin(\psi) \\ \sin(\psi) & \cos(\psi) \end{bmatrix} \tag{11}$$

where $\mathbf{R}(\psi) \in SO(2)$ is the rotation matrix in yaw. When deriving the parameter update laws in Sections 4 and 5 the stability proofs are based on the assumption that (V_x, V_y) are *constant* in NED. This is the standard "constant parameter assumption" used in adaptive control. However, the adaptive control laws will be able to track time-varying currents (V_x, V_y) since the dynamics of the current is slow compared to the system dynamics (time-scale separation) as shown in the simulation study in Section 5.

The equations of relative motion are derived by time differentiating (5). Moreover,

$$\begin{aligned} \dot{y}_e = &-(\dot{x} - \dot{x}_p(\theta)) \sin(\gamma_p) + (\dot{y} - \dot{y}_p(\theta)) \cos(\gamma_p) \\ &- [(x - x_p(\theta)) \cos(\gamma_p) + (y - y_p(\theta)) \sin(\gamma_p)] \, \dot{\gamma}_p \end{aligned} \tag{12}$$

The last bracket in (12) is zero as seen from (4) and

$$\dot{x}_p(\theta) \sin(\gamma_p) - \dot{y}_p(\theta) \cos(\gamma_p) = 0 \tag{13}$$

according to (6). Consequently, (8), (9) and (12) give:

$$\begin{aligned} \dot{y}_e &= -\dot{x} \sin(\gamma_p) + \dot{y} \cos(\gamma_p) \\ &= -(u_r \cos(\psi) - v_r \sin(\psi) + V_x) \sin(\gamma_p) + (u_r \sin(\psi) + v_r \cos(\psi) + V_y) \cos(\gamma_p) \end{aligned} \tag{14}$$

This can be written in *amplitude-phase form*:

$$\dot{y}_e = U_r \sin(\psi + \beta_r - \gamma_p) + U_c \sin(\beta_c - \gamma_p) \tag{15}$$

where the relative speed and direction are recognized as $U_r = \sqrt{u_r^2 + v_r^2}$ and $\beta_r = \text{atan2}(v_r, u_r)$, respectively. Similar, $U_c = \sqrt{u_c^2 + v_c^2}$ and $\beta_c = \text{atan2}(V_y, V_x)$. From the *reverse triangle inequality* if follows that the body-fixed velocities, $\mathbf{v} = [u, v]^\top$, satisfy:

$$\|\mathbf{v}_r\| = \|\mathbf{v} - \mathbf{v}_c\| \geq \|\mathbf{v}\| - \|\mathbf{v}_c\| \tag{16}$$

Since normal operation of a vehicle implies that the vehicle is moving faster than the current, $U > U_c$. Consequently, the relative velocity satisfies:

$$U_r \geq U - U_c > 0 \tag{17}$$

This property will be exploited when designing the adaptive integral LOS guidance laws.

2.3. Integral LOS guidance law

The marine craft LOS algorithms for path following are usually employed at a kinematic level where the goal is to prescribe a value ψ_d for the heading angle ψ in (15). The hydro-acoustic reference system measure U_r, β_r and the cross-track error y_e. Since, the path tangential angle γ_p is known,

DOI: 10.1002/acs

we choose:

$$\psi_d = \gamma_p - \beta_r + \tan^{-1}\left(-\frac{1}{\Delta}(y_e + \alpha_y)\right) \tag{18}$$

where $\Delta > 0$ is the user specified look-ahead distance and α_y is a *virtual control input*, which can be designed to obtain integral action. The virtual control input is not a physical control input but only a design variable used to shape the closed-loop dynamics of the system and to add integral action for compensation of drift forces.

The heading angle tracking error is denoted as:

$$\tilde{\psi} = \psi - \psi_d \tag{19}$$

Substituting (18) into (15) gives:

$$\dot{y}_e = U_r \sin\left(\tilde{\psi} + \tan^{-1}\left(-\frac{1}{\Delta}(y_e + \alpha_y)\right)\right) + U_c \sin(\beta_c - \gamma_p) \tag{20}$$

The kinematic property: $\sin(a+b) = \sin(a)\cos(b) + \cos(a)\sin(b)$, gives:

$$\begin{aligned}\dot{y}_e \quad = \quad & U_r \sin(\tilde{\psi}) \cos\left(\tan^{-1}\left(-\frac{1}{\Delta}(y_e + \alpha_y)\right)\right) + U_r \cos(\tilde{\psi}) \sin\left(\tan^{-1}\left(-\frac{1}{\Delta}(y_e + \alpha_y)\right)\right) \\ & + U_c \sin(\beta_c - \gamma_p)\end{aligned} \tag{21}$$

which reduces to

$$\dot{y}_e = U_r \sin(\tilde{\psi}) \frac{\Delta}{\sqrt{\Delta^2 + (\alpha_y + y_e)^2}} + U_r \cos(\tilde{\psi}) \frac{\alpha_y + y_e}{\sqrt{\Delta^2 + (\alpha_y + y_e)^2}} + U_c \sin(\beta_c - \gamma_p) \tag{22}$$

This can be rewritten as

$$\dot{y}_e = -\frac{U_r(\alpha_y + y_e)}{\sqrt{\Delta^2 + (\alpha_y + y_e)^2}} + U_c \sin(\beta_c - \gamma_p) + U_r \phi(y_e, \tilde{\psi})\tilde{\psi} \tag{23}$$

where

$$\phi(y_e, \tilde{\psi}) := \frac{\sin(\tilde{\psi})}{\tilde{\psi}} \frac{\Delta}{\sqrt{\Delta^2 + (\alpha_y + y_e)^2}} + \frac{\cos(\tilde{\psi}) + 1}{\tilde{\psi}} \frac{(\alpha_y + y_e)}{\sqrt{\Delta^2 + (\alpha_y + y_e)^2}} \tag{24}$$

Property 1 (Boundedness of $\phi(y_e, \tilde{\psi})$)
Assume that $|\alpha_y| \leq \alpha_{\max}$ and $0 < \Delta_{\min} \leq \Delta \leq \Delta_{\max}$. Hence, the function $|\phi(y_e, \tilde{\psi})| \leq c$ for all y_e and $\tilde{\psi}$ since $|\sin(x)/x| \leq 1$, $|(\cos(x) - 1)/x| < 0.73$ for all x and

$$\left|\frac{\Delta}{\sqrt{\Delta^2 + (\alpha_y + y_e)^2}}\right| \leq 1, \quad \left|\frac{\alpha_y + y_e}{\sqrt{\Delta^2 + (\alpha_y + y_e)^2}}\right| \leq 1 \tag{25}$$

Moreover, $c = 1.73$ will be an upper bound for $|\phi(y_e, \tilde{\psi})|$.

3. HEADING AUTOPILOT DESIGN

The yaw dynamics of a marine craft is usually modeled by using the Nomoto model (Fossen [11])

$$\dot{\psi} = r \tag{26}$$

$$T\dot{r} + r = K\delta + b_0 \tag{27}$$

DOI: 10.1002/acs

where T and K are the Nomoto time and gain constants, respectively and $|b_0| \leq b_{\max}$ is a bias term due to environmental disturbances and unmodeled dynamics. For simplicity a single rudder is used to steer the vehicle. The rudder angle is denoted δ. The Nomoto model can easily be modified to include other actuators. Define a sliding surface:

$$s_0 := \tilde{\psi} + \lambda \int_0^t \tilde{\psi}(\tau) d\tau \tag{28}$$

where $\lambda > 0$ is a design constant. Hence,

$$s = \dot{s}_0 + \lambda s_0 = \dot{\tilde{\psi}} + 2\lambda\tilde{\psi} + \lambda^2 \int_0^t \tilde{\psi}(\tau) d\tau \tag{29}$$

represents a sliding surface. The error dynamics can be expressed in state-space form as:

$$\begin{bmatrix} \dot{\tilde{\psi}} \\ \dot{s}_0 \end{bmatrix} = \underbrace{\begin{bmatrix} -\lambda & -\lambda \\ 0 & -\lambda \end{bmatrix}}_{\mathbf{A}} \begin{bmatrix} \tilde{\psi} \\ s_0 \end{bmatrix} + \underbrace{\begin{bmatrix} 1 \\ 1 \end{bmatrix}}_{\mathbf{b}} s \tag{30}$$

It is convenient to define the signal $r_r := r - s$ and the heading controller as:

$$\delta = \frac{1}{K}\left(T\dot{r}_r + r_r - K_d s - \eta\,\mathrm{sgn}(s)\right) \tag{31}$$

where $\mathrm{sgn}(s)$ is the signum function and $K_d > 0$ is the autopilot feedback gain, which is used to add damping and speed up the convergence of the tracking error s to zero. The gain requirement for η is determined by Lyapunov stability analysis. Since,

$$T\dot{s} + (1 + K_d)s + \eta\,\mathrm{sgn}(s) = b_0 \tag{32}$$

we propose the Lyapunov function candidate:

$$V_1 = \mathbf{x}^\top \mathbf{P}\mathbf{x} + \frac{1}{2}Ts^2 \tag{33}$$

where $\mathbf{x} = [\tilde{\psi}, s_0]^\top$ and $\mathbf{P} = \mathbf{P}^\top > 0$ is given by

$$\mathbf{P}\mathbf{A} + \mathbf{A}^\top\mathbf{P} = -q\mathbf{I}_2 \tag{34}$$

for an user specified $q > 0$. Time differentiation of V_1 and substitution of (30) and (32) into the expression for $\dot{V}_1$ under the assumption that $\eta \geq b_{\max}$ gives

$$\begin{aligned} \dot{V}_1 &= -q\mathbf{x}^\top\mathbf{x} + 2\mathbf{x}^\top\mathbf{P}\mathbf{b}s - (1 + K_d)s^2 + b_0 s - \eta|s| \\ &\leq -q||\mathbf{x}||^2 + 2||\mathbf{P}||\,||\mathbf{x}||\,|s| - (1 + K_d)s^2 \end{aligned} \tag{35}$$

Let $\lambda_{\max}(\mathbf{P})$ denote the maximum eigenvalue of $\mathbf{P}$. Hence, the matrix

$$\begin{bmatrix} q & -\lambda_{\max}(\mathbf{P}) \\ -\lambda_{\max}(\mathbf{P}) & 1 + K_d \end{bmatrix} > 0 \tag{36}$$

for $K_d > \lambda_{\max}(\mathbf{P})^2/q - 1 > 0$. This particular choice for K_d implies that $\dot{V}_1 < 0$ and consequently the equilibrium point $[\tilde{\psi}, s_0, s]^\top = \mathbf{0}$ is globally exponentially stable (GES) according to Theorem 4.10 in Khalil [17].

Discussion: The Lyapunov stability analysis gives gain requirements for K_d and η. It is well known that the gain requirements are very conservative. Hence, in practice it is common to treat K_d and η as tunable parameters and just use the Lyapunov function as a tool to choose the structure of the control law (31) such that the origin of the closed-loop system is rendered exponentially stable. Hence, the bounds on the tunable gains have to be viewed as theoretical conservative numbers not needed for practical implementation. Nevertheless, it is easy to satisfy the gain requirements for K_d and η for a marine craft described by the Nomoto model.

DOI: 10.1002/acs

4. STRAIGHT-LINE PATH FOLLOWING

The heading autopilot of Section 3 can be used in cascade with an adaptive LOS guidance law for path following. Consider a straight-line path for which $\gamma_p = \text{constant}$ and define the lateral velocity:

$$\theta_y := U_c \sin(\beta_c - \gamma_p) = \text{constant} \tag{37}$$

as the unknown parameter to be estimated. Consequently, the cross-track error (23) forms a cascade with the heading autopilot system in Section 3:

$$\Sigma_1: \quad \dot{y}_e = \underbrace{-\frac{U_r(y_e + \alpha_y)}{\sqrt{\Delta^2 + (y_e + \alpha_y)^2}}}_{f_1(t, y_e)} + \underbrace{U_r \phi(y_e, \tilde{\psi})}_{g(t, y_e, \tilde{\psi})} \tilde{\psi} + \theta_y \tag{38}$$

$$\Sigma_2: \quad \dot{\tilde{\psi}} = f_2(t, \tilde{\psi}) \tag{39}$$

where $f_2(t, \tilde{\psi})$ defines the yaw angle error dynamics corresponding to (30) and (32). The stability properties of the nonlinear system (38)–(39) are given by Lemma 1:

Lemma 1 (Unforced cascaded system ($\theta_y = 0$))
Assume that ψ_d is computed using (18) and that (31) is used for heading control. Furthermore assume that $U > U_c$ and that $0 < \Delta_{\min} \leq \Delta \leq \Delta_{\max}$. Then the equilibrium point $(y_e, \tilde{\psi}) = (0, 0)$ of the unforced system (38)–(39), that is $\theta_y = 0$, with a bounded virtual control signal α_y is globally $\kappa-$exponentially stable.

Proof
From Section 3 we have that the equilibrium point $\tilde{\psi} = 0$ of the heading autopilot system Σ_2 given by (39) is GES. The equilibrium point $y_e = 0$ of the nominal system (Σ_1-system with $\tilde{\psi} = 0$):

$$\dot{y}_e = -\frac{U_r(y_e + \alpha_y)}{\sqrt{\Delta^2 + (y_e + \alpha_y)^2}} \tag{40}$$

is UGAS and ULES or global $\kappa-$exponential stable as defined by Sørdalen and Egeland [25]. This follows from $V_2 = (1/2)y_e^2$, which after time differentiation along the trajectories of y_e gives:

$$\dot{V}_2 = -\frac{U_r}{\sqrt{\Delta^2 + (y_e + \alpha_y)^2}} y_e^2 \leq 0 \tag{41}$$

Since $U > U_c$, the relative velocity $U_r > 0$. Finally, the linear growth rate condition $|\phi(y_e, \tilde{\psi})| \leq c$ (see Property 1) implies that all conditions of Lemma 8 in Panteley et al. [21] are satisfied and the cascade Σ_1–Σ_2 is globally $\kappa-$exponentially stable. □

4.1. *Indirect adaptive control*

In this section we propose an adaptive disturbance observer, which can estimate the unknown parameter θ_y in (38) due to ocean currents. The observer can be combined with a virtual control input α_y to obtain asymptotic tracking, see Figure 2.

Theorem 1 (Adaptive disturbance observer)
Assume that ψ_d is computed using (18) and that (31) is used for heading control. Furthermore assume that α_y is bounded and that $U > U_c$. Then the adaptive observer:

$$\dot{\hat{y}}_e = -\frac{U_r(\hat{y}_e + \alpha_y)}{\sqrt{\Delta^2 + (y_e + \alpha_y)^2}} + \hat{\theta}_y + K_1(y_e - \hat{y}_e) \tag{42}$$

$$\dot{\hat{\theta}}_y = K_2(y_e - \hat{y}_e) \tag{43}$$

with $0 < \Delta_{\min} \leq \Delta \leq \Delta_{\max}$, and adaptation gains $K_1 > 0$ and $K_2 > 0$ renders the equilibrium point $(\tilde{\psi}, \tilde{y}_e, \tilde{\theta}_y) = (\psi - \psi_d, y_e - \hat{y}_e, \theta_y - \hat{\theta}_y) = (0, 0, 0)$ globally $\kappa-$exponentially stable.

DOI: 10.1002/acs

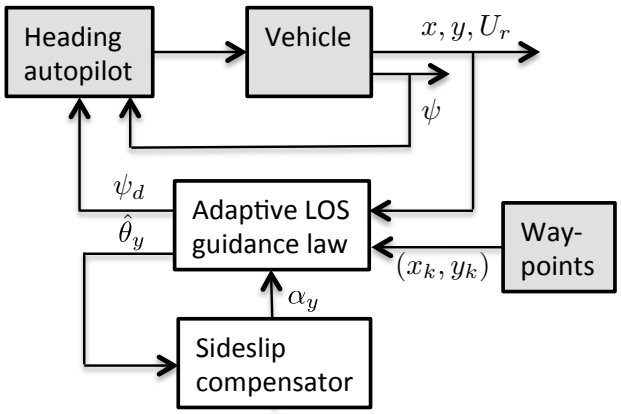

Figure 2. Adaptive integral LOS guidance law and heading autopilot.

Proof
The observer error dynamics for the systems (38)–(39) and (42)–(43) is a cascaded system:

$$\Sigma_1^* : \begin{cases} \dot{\tilde{y}}_e = -\frac{U_r}{\sqrt{\Delta^2+(y_e+\alpha_y)^2}}\tilde{y}_e + \tilde{\theta}_y - K_1\tilde{y}_e + U_r\phi(y_e,\tilde{\psi})\tilde{\psi} \\ \dot{\tilde{\theta}}_y = -K_2\tilde{y}_e \end{cases} \tag{44}$$

$$\Sigma_2 : \quad \dot{\tilde{\psi}} = f_2(t,\tilde{\psi}) \tag{45}$$

where $\dot{\tilde{\theta}}_y = -\dot{\hat{\theta}}_y$. The heading autopilot of Section 3 renders the equilibrium point $\tilde{\psi} = 0$ of the subsystem Σ_2 GES. For the first subsystem Σ_1^* we consider the nominal system:

$$\dot{\tilde{y}}_e = -\frac{U_r}{\sqrt{\Delta^2+(y_e+\alpha_y)^2}}\tilde{y}_e + \tilde{\theta}_y - K_1\tilde{y}_e \tag{46}$$

$$\dot{\tilde{\theta}}_y = -K_2\tilde{y}_e \tag{47}$$

In order to proof stability of (46)–(47) let $V_3 = (1/2)\tilde{y}_e^2 + 1/(2K_2)\tilde{\theta}_y^2$ be a Lyapunov function candidate. Consequently,

$$\begin{aligned} \dot{V}_3 &= -\frac{U_r\tilde{y}_e^2}{\sqrt{\Delta^2+(y_e+\alpha_y)^2}} - K_1\tilde{y}_e^2 + \tilde{\theta}_y\left(\tilde{y}_e + \frac{1}{K_2}\dot{\tilde{\theta}}_y\right) \\ &= -\left(\frac{U_r}{\sqrt{\Delta^2+(y_e+\alpha_y)^2}} + K_1\right)\tilde{y}_e^2 \\ &\leq 0 \end{aligned} \tag{48}$$

Since $U_r > 0$ the signals $\tilde{\theta}_y$ and $\tilde{y}_e$ are bounded. In addition, the equilibrium point $(\tilde{y}_e, \tilde{\theta}_y) = (0,0)$ of (46)–(47) is UGAS/ULES (global $\kappa-$exponential stable). This is seen by writing the error dynamics (46)–(47) in the following form:

$$\dot{x}_1 = f(t,x_1) + g(t,\mathbf{x})x_2 \tag{49}$$

$$\dot{x}_2 = -K_2 g(t,\mathbf{x})x_1 \tag{50}$$

where $x_1 = \tilde{y}_e$, $x_2 = \tilde{\theta}_y$, $\mathbf{x} = [x_1, x_2]^\top$ and

$$f(t,x_1) = -\left(\frac{U_r}{\sqrt{\Delta^2+(y_e+\alpha_y)^2}} + K_1\right)x_1 \tag{51}$$

$$g(t,\mathbf{x}) = 1 \tag{52}$$

DOI: 10.1002/acs

Since $g^2(t,\mathbf{x}) = 1 > 0$, the *persistency of excitation* condition is satisfied and consequently all conditions of Theorem 1 in Fossen et al. [15] (alternatively Panteley et al. [22]) are satisfied. Then we have proven that the nominal system (46)–(47) corresponding to Σ_1^* is globally $\kappa-$exponentially stable. In addition the subsystem Σ_2 is GES and the linear growth rate condition $|\phi(y_e,\tilde{\psi})| \leq c$ (see Property 1) is satisfied for subsystem Σ_1^*. Consequently, all conditions of Lemma 8 in Panteley et al. [21] are satisfied and it follows that the cascade Σ_1^*–Σ_2 is globally $\kappa-$exponentially stable. □

Corollary 1 (Indirect adaptive control and asymptotic tracking)
The adaptive observer (42)–(43) can be used together with a virtual control signal α_y for cancellation of the drift term θ_y in (38) asymptotically. Let the control objective be to drive $y_e \to 0$ when $\hat{\theta}_y \to \theta_y$. From (38) it is seen that perfect asymptotic tracking $y_e = \tilde{\psi} = 0$ and cancellation of θ_y are obtained for:

$$\alpha_y = \Delta \frac{\hat{\theta}_y/U_r}{\sqrt{1-(\hat{\theta}_y/U_r)^2}} \tag{53}$$

Remark 1
The signal $|\hat{\theta}_y/U_r| < 1$ should be saturated in a practical implementation for instance by using a projection algorithm. Let $M_\theta > 0$ be a known constant such that $|\theta_y| \leq M_\theta < U_r$. Hence, the parameter adaptation law (43) can be modified according to: †

$$\dot{\hat{\theta}}_y = \mathrm{Proj}(\hat{\theta}_y, K_2(y_e - \hat{y}_e)) \tag{54}$$

where $|\hat{\theta}_y(0)| \leq M_{\hat{\theta}}$. Hence, the estimate $|\hat{\theta}_y| < U_r$. The projection algorithm does not satisfy the UGAS property of Theorem 1 but global convergence can be proven by applying Barbălat's lemma (Lemma 8.2 in Khalil [17]).

4.2. *Direct adaptive control*

A direct adaptive controller can be designed such that the virtual control input α_y cancels the unknown ocean current θ_y in (38). According to Lemma 1 the cross-track error y_e goes to zero exponentially for the unforced system Σ_1. The velocity parameter θ_y in (38) can be cancelled by choosing α_y such that:

$$\frac{\alpha_y}{\sqrt{\Delta^2+(y_e+\alpha_y)^2}} = \frac{\hat{\theta}_y}{U_r} \tag{55}$$

Solving for α_y gives one feasible solution (the negative root) given by:

$$\alpha_y = \frac{y_e(\hat{\theta}_y/U_r)^2 - (\hat{\theta}_y/U_r)\sqrt{\Delta^2\left(1-(\hat{\theta}_y/U_r)^2\right)+y_e^2}}{1-(\hat{\theta}_y/U_r)^2} \tag{56}$$

Hence, the requirement $|\hat{\theta}_y/U_r| < 1$ must be enforced to ensure that α_y is bounded when estimating θ_y. Consider (38) in the form:

$$\dot{y}_e = -\frac{U_r y_e}{\sqrt{\Delta^2+(y_e+\alpha_y)^2}} - \frac{U_r \alpha_y}{\sqrt{\Delta^2+(y_e+\alpha_y)^2}} + (\tilde{\theta}_y + \hat{\theta}_y) + U_r\phi(y_e,\tilde{\psi})\tilde{\psi} \tag{57}$$

where $\tilde{\theta}_y = \theta_y - \hat{\theta}_y$. If we choose α_y as (56), the cross-track error (57) becomes:

$$\dot{y}_e = -\frac{U_r y_e}{\sqrt{\Delta^2+(y_e+\alpha_y)^2}} + \tilde{\theta}_y + U_r\phi(y_e,\tilde{\psi})\tilde{\psi} \tag{58}$$

† $\mathrm{Proj}(\cdot,\cdot)$ denotes a parameter projection (Krstic et al. [18], App. E), which ensures that $|\theta_y|$ remains smaller than some design constant $M_{\hat{\theta}} > M_\theta$. The details of the parameter projection are given in Appendix A.

DOI: 10.1002/acs

Theorem 2 (Adaptive integral LOS guidance law)
Assume that ψ_d is computed using (18) and (56), and that (31) is used for heading control. Furthermore, assume that $\gamma > 0$, $0 < \Delta_{\min} \leq \Delta \leq \Delta_{\max}$, $U_r > 0$ and that the ocean current is constant and there exists a known constant $M_\theta > 0$ such that $|\theta_y| \leq M_\theta < U_r$. Hence, the parameter adaptation law:

$$\dot{\hat{\theta}}_y = \text{Proj}(\hat{\theta}_y, -\gamma y_e) \tag{59}$$

where $|\hat{\theta}(_y 0)| \leq M_{\hat{\theta}}$ ensures that $y_e \to 0$, $\tilde{\psi} \to 0$ and that $\tilde{\theta}_y$ is bounded.

Proof
Eq. (58) is forced by $\tilde{\theta}_y$. From Lemma 1 it follows that the equilibrium point $(y_e, \tilde{\psi}) = (0, 0)$ of the unforced system, that is the nominal system:

$$\dot{y}_e = -\frac{U_r}{\sqrt{\Delta^2 + (y_e + \alpha_y)^2}} y_e + U_r \phi(y_e, \tilde{\psi}) \tilde{\psi} \tag{60}$$

$$\dot{\tilde{\psi}} = f_2(t, \tilde{\psi}) \tag{61}$$

is globally κ-exponentially stable. Next, the forcing term is included in the analysis by writing (58) and (59) as a cascade. Let $\mathbf{z} = [z_1, z_2]^\top = [y_e, \tilde{\psi}]^\top$. Hence, (58)–(59) can be written:

$$\Sigma_{1p} : \dot{\mathbf{z}} = \mathbf{F}(t, \mathbf{z}) + \mathbf{G}\tilde{\theta}_y \tag{62}$$

$$\Sigma_{2p} : \dot{\tilde{\theta}}_y = -\text{Proj}(\hat{\theta}_y, -\gamma y_e) \tag{63}$$

where

$$\mathbf{F}(t, \mathbf{z}) := \begin{bmatrix} -\frac{U_r}{\sqrt{\Delta^2 + (z_1 + \alpha_y)^2}} z_1 + U_r \phi(\mathbf{z}) z_2 \\ f_2(t, z_2) \end{bmatrix}, \quad \mathbf{G} := \begin{bmatrix} 1 \\ 0 \end{bmatrix} \tag{64}$$

In order to proof stability of (62)–(63) let $V_4 = (1/2)\mathbf{z}^\top \mathbf{z} + 1/(2\gamma)\tilde{\theta}_y^2$ with $\gamma > 0$ be a Lyapunov function candidate. Consequently,

$$\dot{V}_4 = \mathbf{z}^\top \left(\mathbf{F}(t, \mathbf{z}) + \mathbf{G}\tilde{\theta}_y \right) + \frac{1}{\gamma} \tilde{\theta}_y \dot{\tilde{\theta}}_y \tag{65}$$

Since $\dot{\tilde{\theta}}_y = \dot{\theta}_y - \dot{\hat{\theta}}_y = -\text{Proj}(\hat{\theta}_y, -\gamma y_e)$ and Lemma 1 guarantees that $\mathbf{z}^\top \mathbf{F}(t, \mathbf{z}) \leq 0$ it follows that:

$$\begin{aligned} \dot{V}_4 &= \mathbf{z}^\top \mathbf{F}(t, \mathbf{z}) + \tilde{\theta}_y \left(-\frac{1}{\gamma} \text{Proj}(\hat{\theta}_y, -\gamma y_e) + y_e \right) \\ &\leq 0 \end{aligned} \tag{66}$$

where we have exploited the fact that $-\tilde{\theta}_y \text{Proj}(\hat{\theta}_y, \tau) \leq -\tilde{\theta}_y \tau$ (see Appendix A). It can be shown that $\ddot{V}_4$ is bounded and consequently global convergence of $y_e \to 0$ and $\tilde{\psi} \to 0$ as well as boundedness of the parameter estimation error $\tilde{\theta}_y$ follows from Barbălat's lemma (Lemma 8.2 in Khalil [17]). □

DOI: 10.1002/acs

5. CURVED-PATH PATH FOLLOWING

For the curved-path case the path-tangential angle γ_p will be time varying. The results of Theorem 2 can be extended to curved paths by using over-parametrization. Consider the cross-track error (15) in the following form:

$$\begin{aligned}\dot{y}_e &= U_r \sin(\psi - \gamma_p + \beta_r) + U_c \sin(-\gamma_p)\cos(\beta_c) + U_c \cos(-\gamma_p)\sin(\beta_c) \\ &:= U_r \sin(\psi - \gamma_p + \beta_r) + \sin(\gamma_p)\theta_1 + \cos(\gamma_p)\theta_2 \end{aligned} \tag{67}$$

where $\theta_1 := U_c \cos(\beta_c)$ and $\theta_2 := -U_c \sin(\beta_c)$ are two unknown constants. Choosing the desired yaw angle according to (18) gives:

$$\dot{y}_e = -\frac{U_r(y_e + \alpha_y)}{\sqrt{\Delta^2 + (y_e + \alpha_y)^2}} + \sin(\gamma_p)\theta_1 + \cos(\gamma_p)\theta_2 + U_r \phi(y_e, \tilde{\psi})\tilde{\psi} \tag{68}$$

The virtual control input α_y canceling the drift term is chosen as:

$$\frac{\alpha_y}{\sqrt{\Delta^2 + (y_e + \alpha_y)^2}} = \frac{\sin(\gamma_p)\hat{\theta}_1 + \cos(\gamma_p)\hat{\theta}_2}{U_r} := \theta_n \tag{69}$$

where $\hat{\theta}_1$ and $\hat{\theta}_2$ are the parameter estimates, and α_y is computed using a similar approach as (56). Moreover,

$$\alpha_y = \frac{y_e \theta_n^2 - \theta_n \sqrt{\Delta^2(1 - \theta_n^2) + y_e^2}}{1 - \theta_n^2} \tag{70}$$

The parameter update laws are:

$$\dot{\hat{\theta}}_1 = \mathrm{Proj}(\hat{\theta}_1, -\gamma \sin(\gamma_p) y_e) \tag{71}$$

$$\dot{\hat{\theta}}_2 = \mathrm{Proj}(\hat{\theta}_2, -\gamma \cos(\gamma_p) y_e) \tag{72}$$

where $|\hat{\theta}_1(0)| \leq M_{\hat{\theta}}$ and $|\hat{\theta}_2(0)| \leq M_{\hat{\theta}}$ ensure that $|\theta_1|$ and $|\theta_2|$ remain smaller than some design constant $M_{\hat{\theta}} > M_\theta$. The constraint $|\theta_n| < 1$ are satisfied if M_θ is chosen such that $|\theta_i| \leq M_\theta < (1/2)U_r$ for $i = 1, 2$. Again Barbălat's lemma can be used to prove that $\tilde{y}_e$ and $\tilde{\psi}$ go to zero and the signals $\tilde{\theta}_1$ and $\tilde{\theta}_2$ are bounded by following a similar approach as Theorem 2.

6. AUV CASE STUDIES

All three methods developed in Sections 4.1, 4.2 and 5 are simulated under the same conditions in order to evaluate and compare their efficiency and robustness. We have used a small cylinder-shaped AUV (weight 100 kg), which is modeled as a linear mass-damper system in surge, sway and yaw. The goal is to follow a curved path resulting from interpolating with *natural cubic splines* between six waypoints $\mathrm{wpt}_1 = (10, 10)$, $\mathrm{wpt}_2 = (500, 500)$, $\mathrm{wpt}_3 = (900, 900)$, $\mathrm{wpt}_4 = (1000, 1600)$, $\mathrm{wpt}_5 = (800, 2250)$ and $\mathrm{wpt}_6 = (0, 3000)$ where the units are meters (see Figure 3). The case study is set up as two phases:

- *Phase 1:* The vehicle starts at an initial position $(x_0, y_0) = (-40\,\mathrm{m}, 60\,\mathrm{m})$ and heading $\psi_0 = 0$ deg away from the curved path. During the first phase the vehicle moves under the influence of an unknown ocean current with *constant* magnitude and direction ($U_c = 2$ m/s and $\beta_c = 135$ deg) in the NED frame. This phase is completed when the vehicle crosses wpt_4 as shown in Figure 3.
- *Phase 2:* As soon as the vehicle begins to move between wpt_4 and wpt_5, and until the end of the simulation, the ocean current becomes *time-varying* both in magnitude and direction. A stochastic variation within the ranges $1.5 \leq U_c \leq 2.5$ m/s and $125 \leq \beta_c \leq 145$ deg is simulated using a Gaussian model (see Figure 9). The large current speed is chosen for illustration only and smaller AUVs cannot produce thrust of this magnitude.

DOI: 10.1002/acs

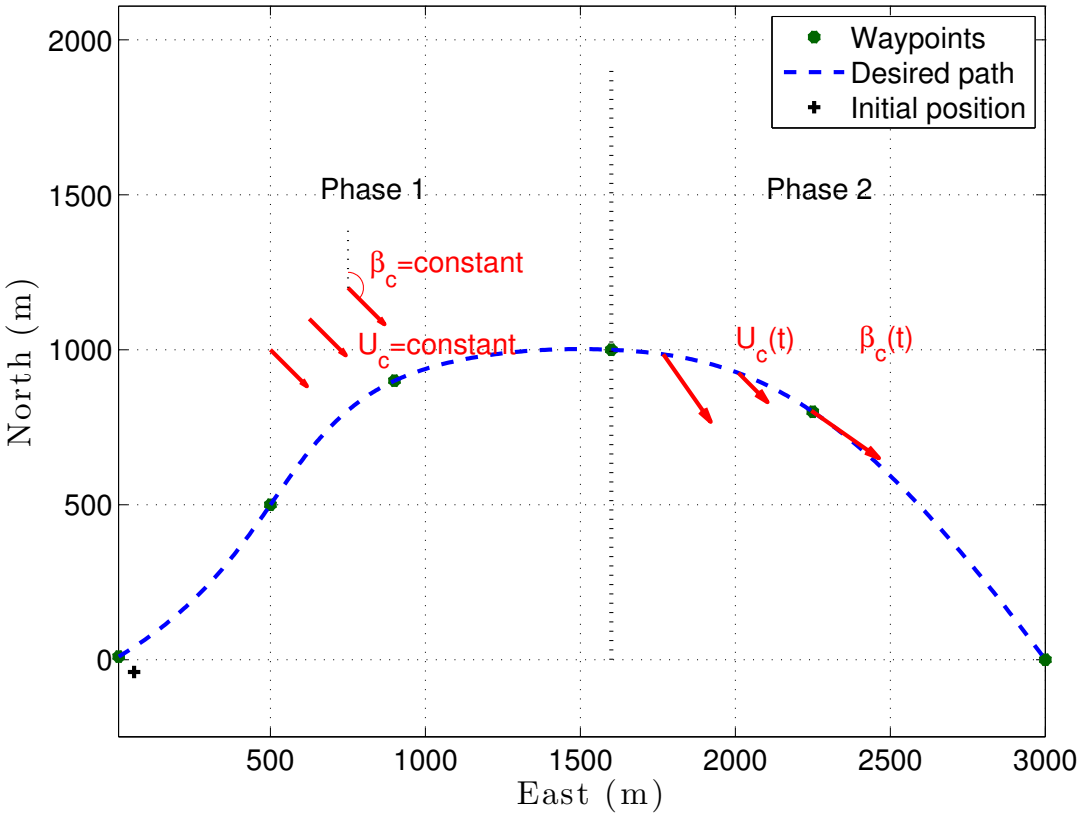

Figure 3. The assigned task consists of two phases: 1) Curved-path path following under the influence of a constant ocean current, and 2) Curved-path path following under the influence of a stochastic ocean current. Phase 2 is initiated right after the vehicle has passed the fourth waypoint.

A P-controller was used to stabilize the forward relative speed at $u_r = 6$ m/s, while the LOS lookahead distance was chosen as $\Delta = 40$ m.

6.1. Case Study 1: Indirect Adaptive LOS

For the indirect adaptive observers, the observer gains were chosen as $K_1 = 10$ and $K_2 = 0.8$. It was assumed that the ocean current was unknown. The observer's initial conditions were chosen as $(\hat{y}_e, \hat{\theta}_y) = (0, 0)$.

Fig. 4 shows that the indirect adaptive LOS eliminates the initial cross-track error of approximately 68 m and manages to keep the vessel on the curved path during both phases. In Fig. 5 the plots of the surge speed and heading angle (desired versus true) of the vehicle are given. The sway velocities as well as the sideslip angles (both relative and absolute) are plotted in Fig. 6. Since the current becomes stochastic after wpt_4, the absolute sway and sideslip angle show a stochastic behavior as well. However, the relative sideslip angle β_r and sway v_r are smooth. The input α_y as well as the ratio $\hat{\theta}_y/U_r$ can be seen in Fig. 7. Finally, Figs. 8–9 depict the ocean current magnitude and direction throughout the whole simulation.

DOI: 10.1002/acs

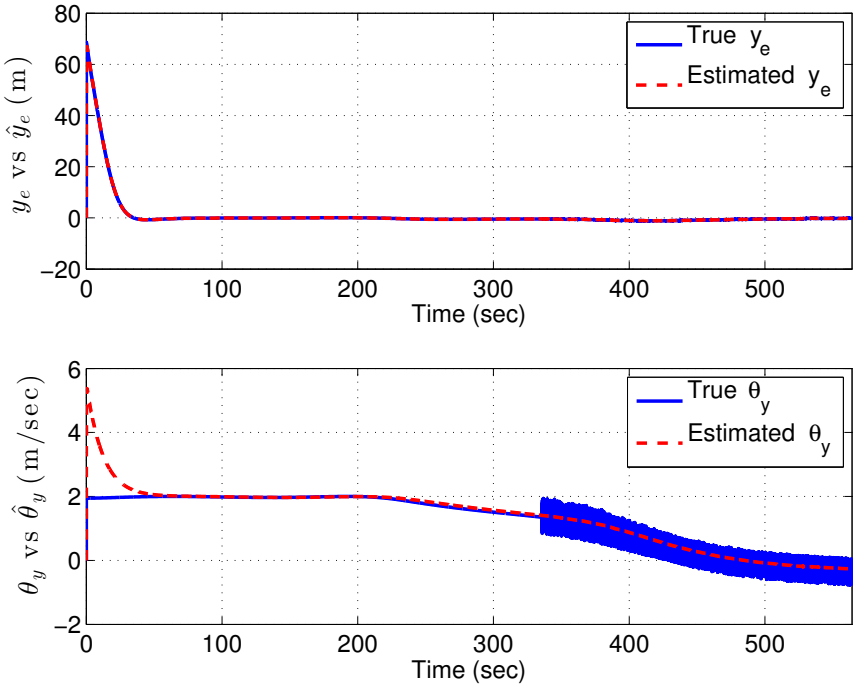

Figure 4. Indirect Adaptive LOS: The cross-track error y_e converges to zero. Moreover, the observer is successful in estimating the current effect in the direction normal to the path, θ_y.

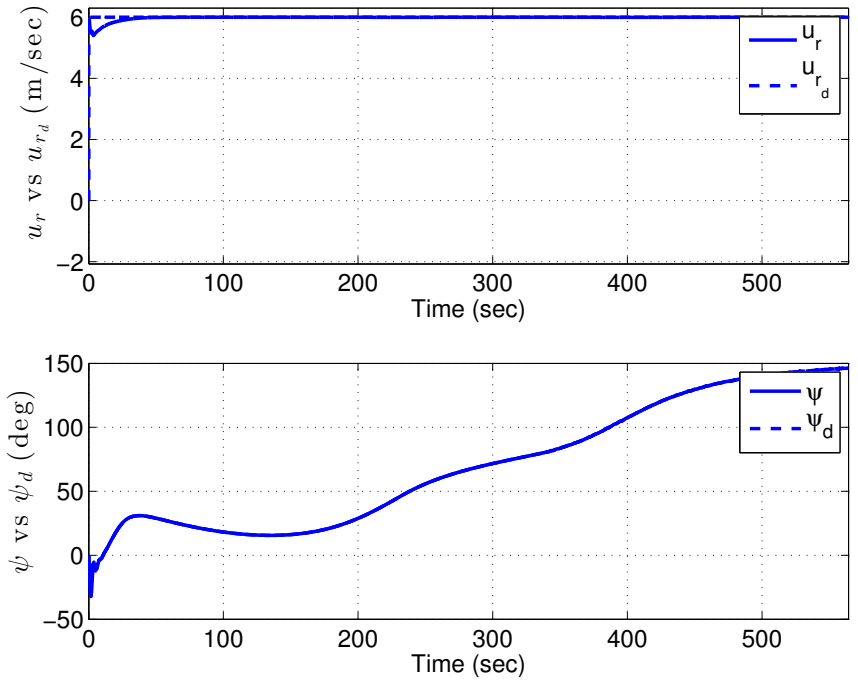

Figure 5. Indirect Adaptive LOS: surge speed and heading angle (desired versus true).

DOI: 10.1002/acs

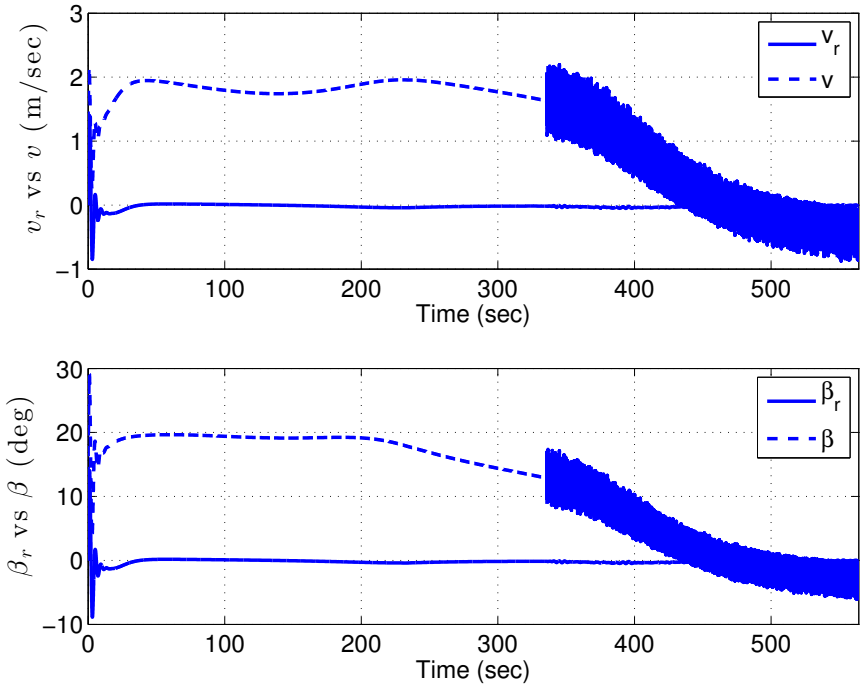

Figure 6. Indirect Adaptive LOS: sway velocities and sideslip angles (relative versus absolute)

.

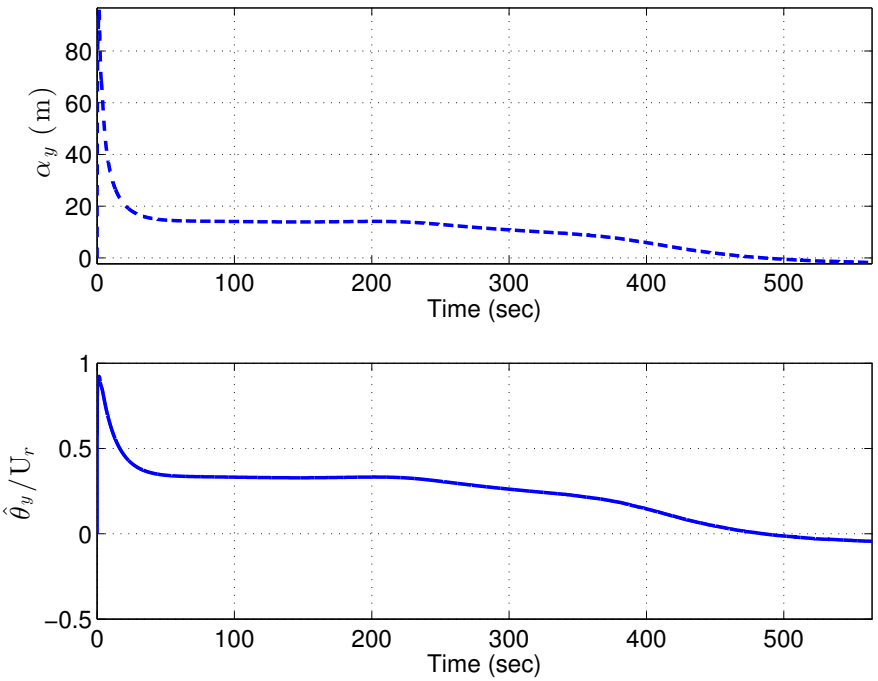

Figure 7. Indirect Adaptive LOS: plots of the bounded virtual control signal α_y and the ratio $\hat{\theta}_y/U_r$. Notice that $|\hat{\theta}_y/U_r| < 1$.

DOI: 10.1002/acs

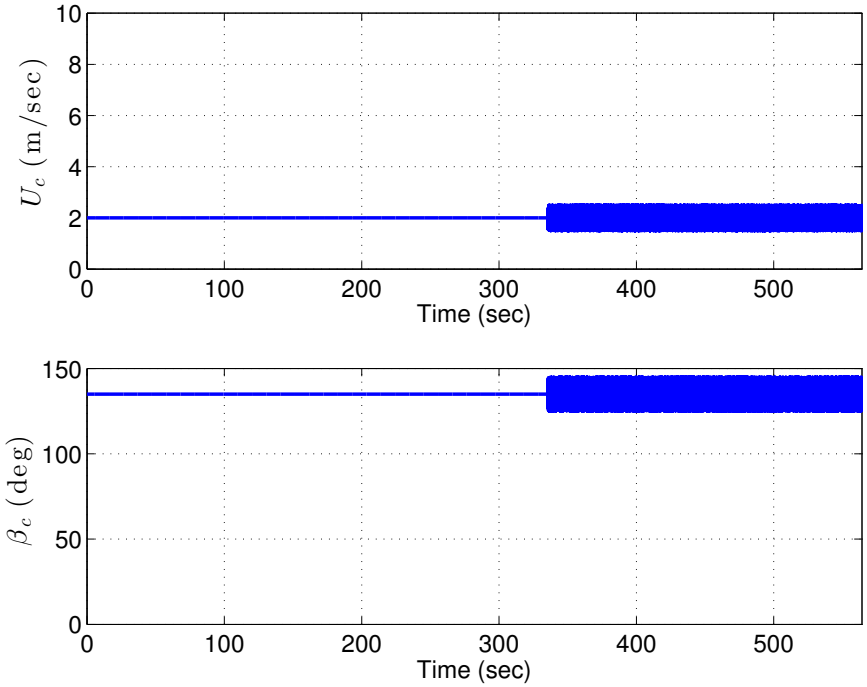

Figure 8. Indirect Adaptive LOS: plots of the current magnitude and direction

.

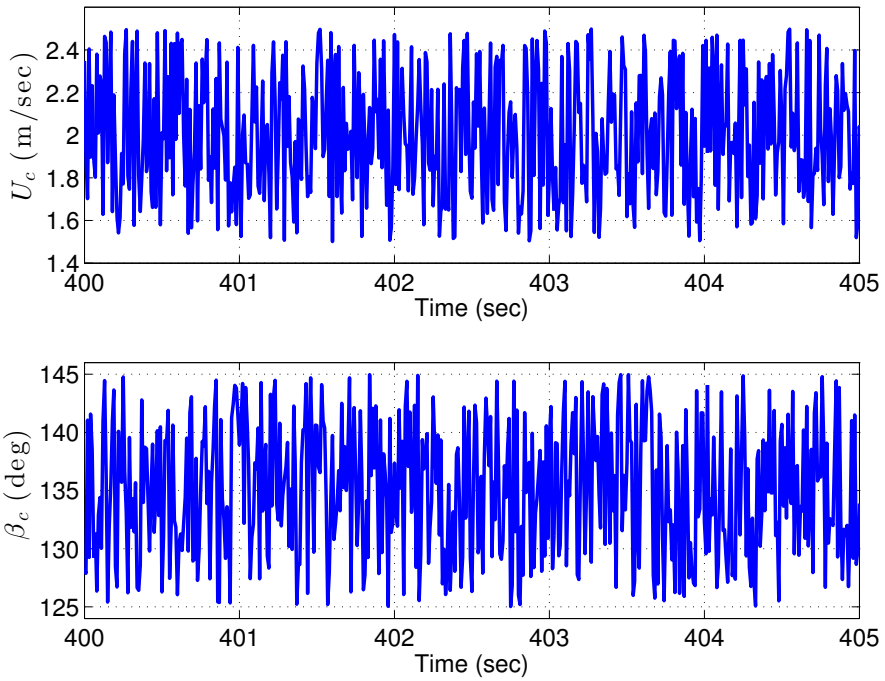

Figure 9. Indirect Adaptive LOS: zoomed plots of the current magnitude and direction showing the stochastic behavior

.

DOI: 10.1002/acs

6.2. *Case Study 2: Direct Adaptive LOS*

The gain for the direct adaptive controller was chosen as $\gamma = 0.15$, while $M_\theta = 2$ and $M_{\hat{\theta}} = 2.01$. The performance of the controller is shown in Figs. 10–13.

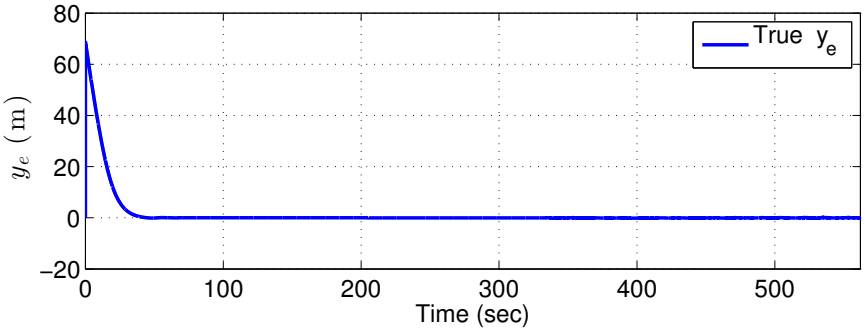

Figure 10. Direct Adaptive LOS: The cross-track error converges to zero

.

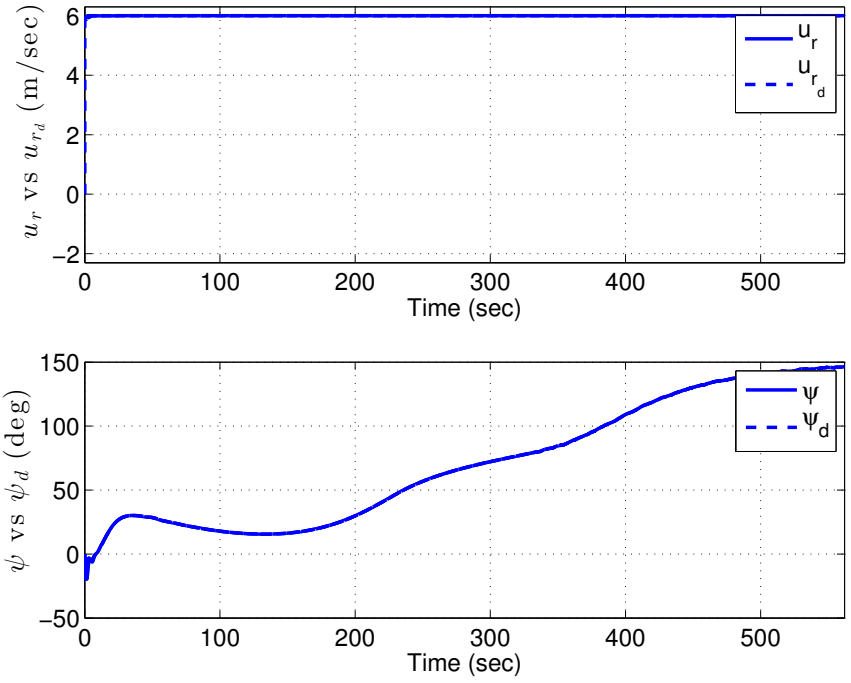

Figure 11. Direct Adaptive LOS: surge speed and heading angle (desired versus true)

.

DOI: 10.1002/acs

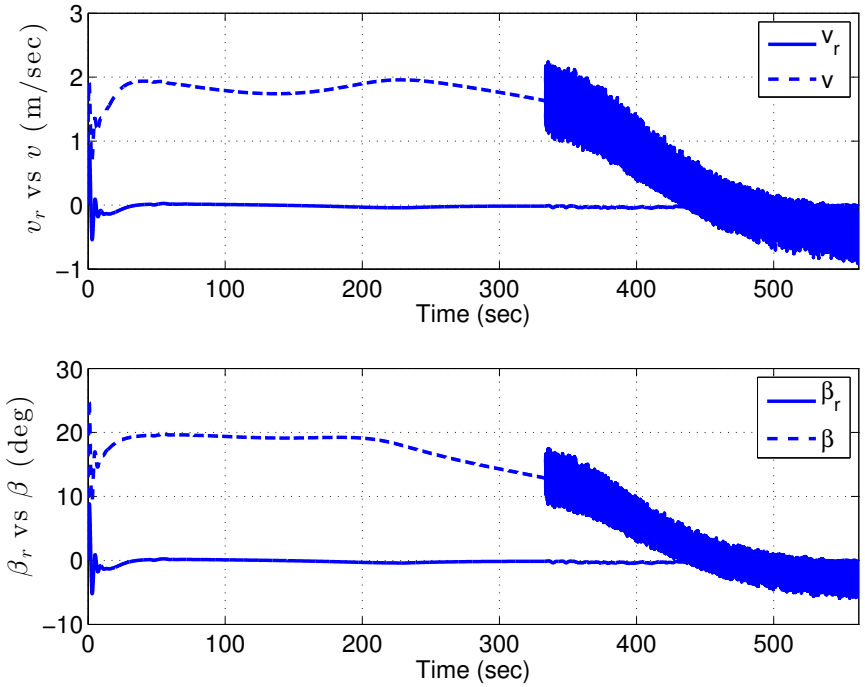

Figure 12. Direct Adaptive LOS: sway velocities and sideslip angles (relative versus absolute)

.

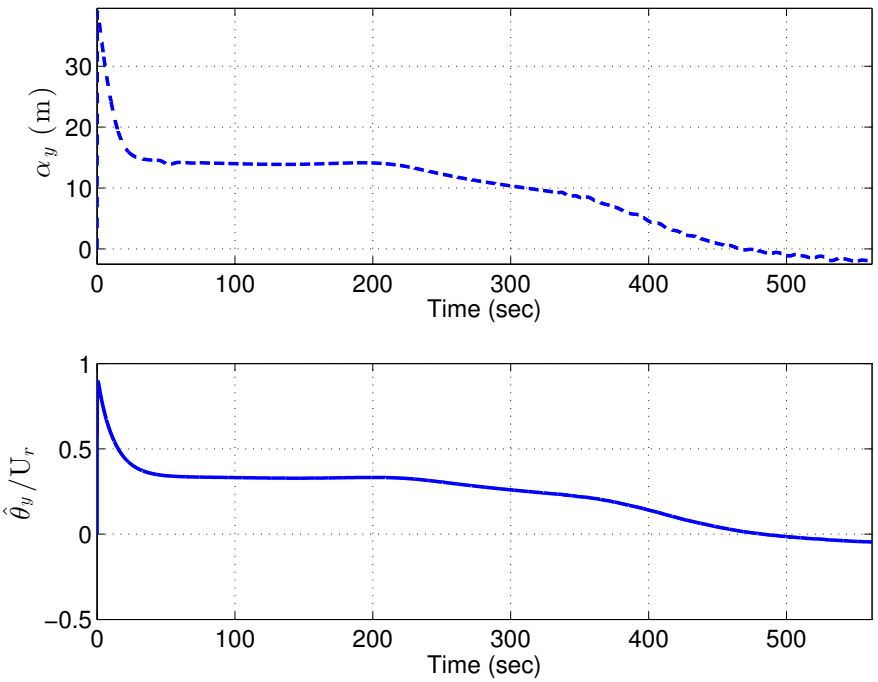

Figure 13. Direct Adaptive LOS: plots of the bounded virtual control signal α_y and the ratio $\hat{\theta}_y/U_r$. Notice that $|\hat{\theta}_y/U_r| < 1$.

.

DOI: 10.1002/acs

6.3. *Case Study 3: Direct Adaptive LOS with Overparametrization*

Similarly to Case Study 2, the gain for the direct adaptive observer was chosen as $\gamma = 0.15$, while $M_{\theta_1} = M_{\theta_2} = 2$ and $M_{\hat{\theta_1}} = M_{\hat{\theta_2}} = 2.01$. The performance of the controller is shown in Figs. 14–17.

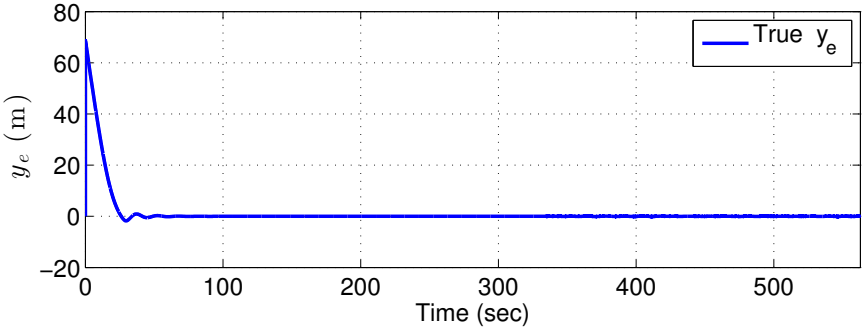

Figure 14. Direct adaptive LOS with overparametrization: The cross-track error converges to zero

.

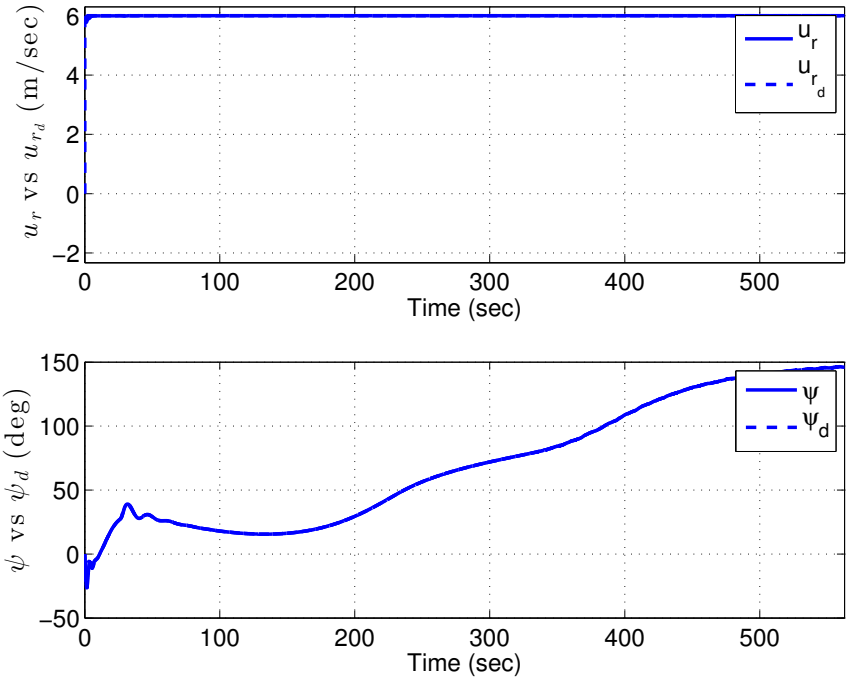

Figure 15. Direct adaptive LOS: surge speed and heading angle (desired versus true)

.

DOI: 10.1002/acs

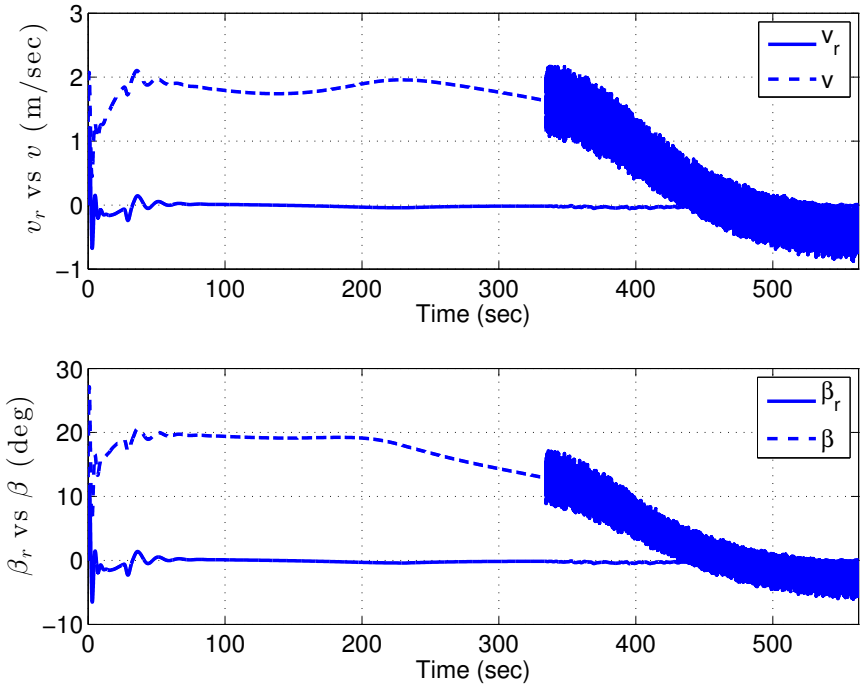

Figure 16. Direct adaptive LOS with overparametrization: sway velocities and sideslip angles (relative versus absolute)

.

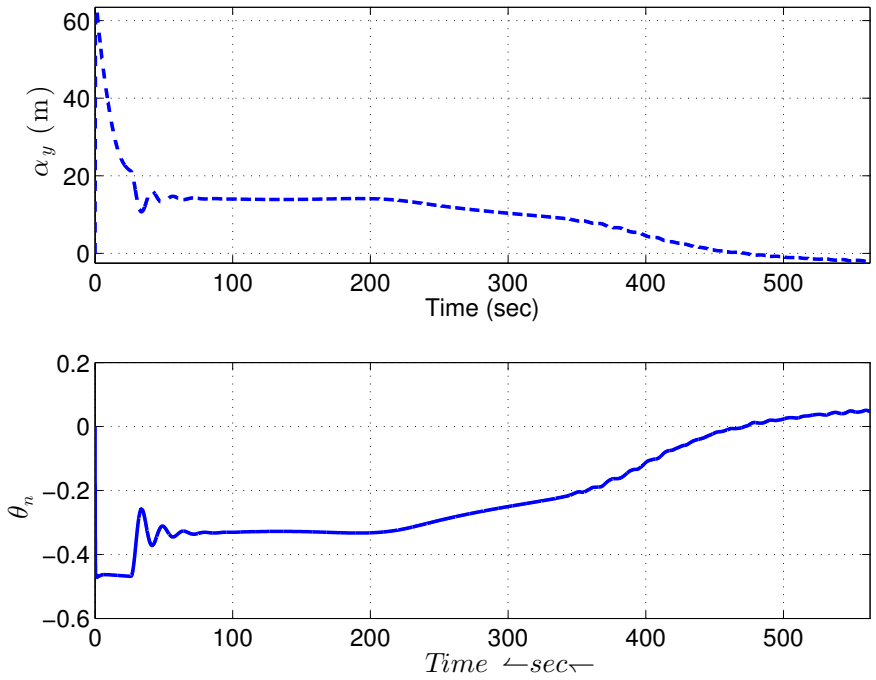

Figure 17. Direct Adaptive LOS with overparametrization: plots of the bounded virtual control signal α_y and the parameter θ_n. Notice that $|\theta_n| < 1$.

.

DOI: 10.1002/acs

7. CONCLUSIONS

Two nonlinear adaptive path-following algorithms for estimation and compensation of ocean currents have been presented: 1) a globally κ-exponentially stable adaptive disturbance observer intended for an indirect adaptive control approach, and 2) a globally convergent direct adaptive control law.

The algorithms are based on a classical LOS guidance principle for marine craft and *integral action* is obtained by parameter adaptation. This resulted in a conceptual new integral LOS guidance law based, which effectively compensate for time-varying drift forces due to waves, wind and ocean currents. The structure of the adaptive integral LOS guidance law is different from the well established integral LOS controller of Børhaug et al. [7]. Both curved- and straight-line path following are considered. An AUV case study verifies the results.

ACKNOWLEDGEMENT

This work was supported by the Norwegian Research Council (project no. 223254) through the Center of Autonomous Marine Operations and Systems (AMOS) at the Norwegian University of Science and Technology (NTNU).

A. PARAMETER PROJECTION

The parameter projection $\mathrm{Proj}(\hat{\theta}_y, \tau)$ used for ocean current estimation is defined as:

$$\mathrm{Proj}(\hat{\theta}_y, \tau) := \begin{cases} \left(1 - c(\hat{\theta}_y)\right)\tau & \text{if } |\hat{\theta}_y| > M_{\hat{\theta}} \text{ and } \hat{\theta}_y \tau > 0 \\ \tau & \text{otherwise} \end{cases} \tag{73}$$

where $c(\hat{\theta}_y) = \min\{1, (\hat{\theta}_y^2 - M_{\hat{\theta}}^2)/(M_{\hat{\theta}}^2 - M_{\theta}^2)\}$. This is a special case of the parameter projection from Appendix E of [18]. The following properties hold for the parameter projection: (i) $\mathrm{Proj}(\hat{\theta}_y, \tau)$ is locally Lipschitz continuous, (ii) $-\tilde{\theta}_y \,\mathrm{Proj}(\hat{\theta}_y, \tau) \leq -\tilde{\theta}_y \tau$.

REFERENCES

1. A. P. Aguiar and J. P. Hespanha. 2007. Trajectory-tracking and path-following of underactuated autonomous vehicles with parametric modeling uncertainty. *IEEE Trans. on Automatic Control*, Vol. 52, No. 8, pp. 1362–1379.
2. M. Aicardi, G. Casalino, G. Indiveri, A. Aguiar, P. Encarnaçao and A. Pascoal. A planar path following controller for underactuated marine vehicles. In: *Proc. 9th Mediterranean Conf. on Control and Automation*, 2001.
3. M. Breivik, V. E. Hovstein and T. I. Fossen. 2008. Straight-line target tracking for unmanned surface vehicles. *Modeling, Identification and Control*, vol. 29, no. 4, pp. 131–149.
4. M. Breivik. 2010. Topics in guided motion control of marine vehicles, Ph.D. dissertation, Norwegian University of Science and Technology, 2010.
5. M. Breivik and T. I. Fossen. 2004. Path following for marine surface vessels, *Proc. of the Offshore Technology Conference (OTC'04)*, Kobe, Japan, 2004, pp. 2282-2289.
6. M. Breivik and T. I. Fossen. 2009. *Guidance laws for autonomous underwater vehicles*. INTECH Education and Publishing, ch. 4, pp. 51-76.
7. E. Børhaug, A. Pavlov, and K. Y. Pettersen. 2008. Integral LOS control for path following of underactuated marine surface vessels in the presence of constant ocean currents, *Proc. IEEE CDC'09, Cancun, Mexico*, pp. 4984-4991.
8. W. Caharija, M. Candeloro, K. Y. Pettersen, and A. J. Sørensen. 2012. Relative velocity control and integral LOS for path following of underactuated surface vessels, *Proc. IFAC MCMC'12*, Arenzano, Italy, 2012.
9. K. D. Do, Z.-P. Jiang and J. Pan. Robust adaptive path following of underactuated ships, *Automatica*, Vol. 40, No. 6, 2004, pp. 929–944.
10. T. I. Fossen, M. Breivik and R. Skjetne. 2003. Line-of-sight path following of underactuated marine craft, *Proc. IFAC MCMC'03, Girona, Spain*, pp. 244-249.
11. T. I. Fossen. 2011. *Handbook of Marine Craft Hydrodynamics and Motion Control*. Wiley.
12. T. I. Fossen, K. Y. Pettersen and R. Galeazzi. Line-of-Sight Path Following for Dubins Paths with Adaptive Sideslip Compensation of Drift Forces. *IEEE Transactions on Control Systems Technology*, 2015.
13. T. I. Fossen and K. Y. Pettersen. 2015. On uniform semiglobal exponential stability (USGES) of proportional line-of-sight guidance laws. *Automatica*, Vol. 50, No. 11, 2014, pp. 2912–2-917.

DOI: 10.1002/acs

14. T. I. Fossen. 2012. How to incorporate wind, waves and ocean currents in the marine craft equations of motion, *Proc. MCMC'12, September, Arenzano, Italy.*
15. T. I. Fossen, A. Loria and A. Teel. 2001. A theorem for UGAS and ULES of (passive) nonautonomous systems: robust control of mechanical systems and ships. *Int. J. of Robust and Nonlinear Control*, Vol. 11:95-108.
16. A. J. Healey and D. Lienard. 1993. Multivariable sliding mode control for autonomous diving and steering of unmanned underwater vehicles *IEEE Journal of Oceanic Engineering*, vol. 18, no. 3, pp. 327–339.
17. H. K. Khalil. 2002. *Nonlinear Systems*. Prentice-Hall.
18. M. Krstic, I. Kanellakopoulos and P. V. Kokotovic. 1995. *Nonlinear and Adaptive Control Design*. Wiley.
19. L. Lapierre, D. Soetanto and A. Pascoal. 2003. Nonlinear path following with applications to the control of autonomous underwater vehicles. In: *Proc. 42nd IEEE Conf. on Decision and Control*, Vol. 2, pp. 1256–1261.
20. A. M. Lekkas and T. I. Fossen. 2013. Line-of-sight guidance for path following of marine vehicles. Chapter 5, In *Advanced in Marine Robotics*, LAP LAMBERT Academic Publishing (O. Gal, Ed.), pp. 63–92.
21. E. Panteley, E. Lefeber, A. Loria and H. Nijmeijer. 1998. Exponential tracking control of mobile car using a cascaded approach. *In :Proceedings of the IFAC Workshop on Motion Control*, Grenoble, France, pp. 221—226.
22. E. Panteley, A. Loria and A. Teel. Relaxed persistency of excitation for uniform asymptotic stability. *IEEE Transactions on Automatic Control*, Vol. 46, No. 12, 2001.
23. C. Samson (1992). Path following and time-varying feedback stabilization of a wheeled mobile robot. In: *Proc. Int. Conf. ICARCV'92*.
24. R. Skjetne, T. I. Fossen and P. V. Kokotovic. 2004. Robust output maneuvering for a class of nonlinear systems. *Automatica*, vol. 40, no. 3, pp. 373-–383.
25. O. J. Sørdalen and O. Egeland. 1995. Exponential stabilization of nonholonomic chained systems. *IEEE Transactions on Automatic Control*, Vol. 40, No. 1.
26. R. Yanushevsky. 2011. *Guidance of Unmanned Aerial Vehicles*. CRC Press.

DOI: 10.1002/acs